Wait's Complex-Image Principle Generalized to Arbitrary Sources

Ismo V. Lindell, *Fellow, IEEE*, Jari J. Hänninen, and Risto Pirjola

***Abstract*—The well-known simple and remarkably accurate approximate low-frequency (LF) complex-image method introduced in 1969 by J. R. Wait to compute the effect of the ground to the field of a divergenceless horizontal current (vertical magnetic current) is generalized to arbitrary current sources through the exact image formulation. The images of a vertical dipole, a horizontal current segment, and an oscillating point charge are first reduced to simplified but asymptotically exact forms and, subsequently, in terms of delta and step-functions to approximate image expressions that also include Wait's image. The novel part of the image is tested numerically through a geophysical example.**

***Index Terms*—Electromagnetic (EM) radiation, low-frequency (LF) radio propagation effects, nonhomogeneous media.**

I. Introduction

SINCE its introduction in 1969 by J. R. Wait [1]–[3], the complex image principle (henceforth, "Wait's image principle") has become very popular for computing geophysical low-frequency (LF) fields due to atmospheric currents and other geo-electromagnetic (EM) sources above the earth. The method is an extension of the classical image principle associated with the perfectly electrically conducting (PEC) plane and it is asymptotically valid when $\omega \to 0$. Wait's image principle is normally presented as the geometric image of the original source in a PEC plane at a complex depth depending on the conductivity of the ground and the frequency. The principle was later extended to the stratified ground by expressing the complex depth in terms of the impedance of the stratified ground [4]. In 1984, an exact form for the image theory was constructed and Wait's image principle was shown to emerge as its asymptotic approximation [5], [19], [20]. In the formalism of the given exact theory the image of a point source is a line source in complex space.

Because Wait's image principle was defined for the vertical magnetic dipole (small horizontal current loop), it can be applied to any horizontal current distributions provided the current is solenoidal, i.e., it satisfies $\nabla \cdot \mathbf{J}(\mathbf{r}) = 0$, and when the frequency is low enough [8]. However, if the divergence of the horizontal current does not vanish, there is accumulation of charge and Wait's image does not give good results. It is the purpose of the present paper to derive an extension to Wait's image principle from an asymptotic limit of the exact image theory given in [10] so that also the charge distribution can be taken into account. Also, an approximate image for the vertical component of the electric current can be obtained. Another complex image principle for vertical currents was recently introduced by replacing it through an equivalent horizontal divergence-free current system [6].

The outline of the paper is as follows. First, we review the basics of the exact image theory for the planar interface and consider its LF asymptotic form when $\omega \to 0$. Next, it is shown that the exact image expressions can be simplified from infinite series of Bessel functions to simple Bessel function formulas which are asymptotically exact in the LF case. Finally, by applying δ and step-function approximation to the image functions, we obtain simple approximative image expressions of which Wait's image is seen to emerge as one example.

Manuscript received September 1, 1999; revised March 6, 2000.

I. V. Lindell and J. J. Hänninen are with the Electromagnetics Laboratory, Helsinki University of Technology, FIN-02015 HUT, Espoo, Finland (e-mail: ismo.lindell@hut.fi).

R. Pirjola is with the Geophysical Research Division, Finnish Meteorological Institute, FIN-00101 Helsinki, Finland.

Publisher Item Identifier S 0018-926X(00)09351-0.

II. Image Theory for the Planar Interface

A. General Expressions

Let us start from the exact image formulation given in [10] as applied to the simple case of current source $\mathbf{J}(\mathbf{r})$ in air above the planar interface of a homogeneous ground with permittivity $\epsilon_r\epsilon_o$ and permeability $\mu_r\mu_o$. The electric field reflected from the ground can be represented as radiated by an image current source in air, $\mathbf{J}_i(\mathbf{r}, \zeta)$, a function of the position vector $\mathbf{r}$ and an integration parameter ζ [10, eq. (7.261)]:

$$\mathbf{E}_r(\mathbf{r}) = -jk_o\eta_o\left(\overline{\overline{I}} + \frac{1}{k_o^2}\nabla\nabla\right) \cdot \int_V \int_0^\infty G(\mathbf{r} - \mathbf{r}' + \mathbf{u}_z\zeta)\mathbf{J}_i(\mathbf{r}', \zeta)\, dV'\, d\zeta. \quad (1)$$

Here, $k_o = \omega\sqrt{\mu_o\epsilon_o}$ denotes the wavenumber and $\eta_o = \sqrt{\mu_o/\epsilon_o}$ the wave impedance in the air region $z > 0$. $G(\mathbf{r})$ is the scalar Green function

$$G(\mathbf{r}) = \frac{e^{-jk_oD(\mathbf{r})}}{4\pi D(\mathbf{r})}, \quad D(\mathbf{r}) = \sqrt{\mathbf{r}\cdot\mathbf{r}}. \quad (2)$$

For complex arguments, the branch of the square root must be taken so that its imaginary part is nonpositive. This makes the Green function exponentially decaying with distance.

According to the original theory, the image source can be expressed in the form [10, eq. (7.257)],

$$\mathbf{J}_i(\mathbf{r}, \zeta) = \left[f^{\mathrm{TM}}(\zeta)\mathbf{u}_z\mathbf{u}_z + f^{\mathrm{TE}}(\zeta)\overline{\overline{I}}_t - \frac{1}{k_o^2}f_o'(\zeta)\mathbf{u}_z\nabla_t\right] \cdot \mathbf{J}_c(\mathbf{r}) \quad (3)$$

$$\mathbf{J}_c(\mathbf{r}) = \overline{\overline{C}}\cdot\mathbf{J}(\overline{\overline{C}}\cdot\mathbf{r}), \quad \overline{\overline{C}} = \overline{\overline{I}} - 2\mathbf{u}_z\mathbf{u}_z = \overline{\overline{I}}_t - \mathbf{u}_z\mathbf{u}_z. \quad (4)$$

The mirror reflection dyadic $\overline{\overline{C}}$ produces the mirror image $\mathbf{J}_c(\mathbf{r})$ of the original source. The three scalar image functions denoted by $f^{\rm TM}(\zeta)$, $f^{\rm TE}(\zeta)$, $f_o'(\zeta)$ (prime denotes differentiation) depend on the electric properties of the ground $z \le 0$. Everywhere, the subscript t denotes a component transverse to the z axis.

To simplify the field expression, let us assume that the original source exists on a horizontal plane at the height $z = h$ above the ground, i.e., that the current function and its mirror image are of the form

$$\mathbf{J}(\mathbf{r}) = \mathbf{J}_s(\boldsymbol{\rho})\delta(z-h), \quad \mathbf{J}_c(\mathbf{r}) = \overline{\overline{C}} \cdot \mathbf{J}_s(\boldsymbol{\rho})\delta(z+h). \tag{5}$$

Here, $\mathbf{J}_s(\boldsymbol{\rho})$ is a surface density source (dimension A/m) which may also have a vertical component. Now the δ function $\delta(z+h)$ can be integrated out in (1), which thus reduces to a threefold integral. Changing the ζ variable to $-z'-h$, (1) can be rewritten as

$$\mathbf{E}_r(\mathbf{r}) = -jk_o\eta_o\left(\overline{\overline{I}} + \frac{1}{k_o^2}\nabla\nabla\right) \cdot \int_V G(\boldsymbol{\rho}-\boldsymbol{\rho}'+\mathbf{u}_z(z-z'))\mathbf{J}_i(\mathbf{r}')\,dV' \tag{6}$$

where the image source is of the form

$$\mathbf{J}_i(\mathbf{r}) = \left[f^{\rm TM}(\zeta)\mathbf{u}_z\mathbf{u}_z + f^{\rm TE}(\zeta)\overline{\overline{I}}_t - \frac{1}{k_o^2}f_o'(\zeta)\mathbf{u}_z\nabla_t\right] \cdot \overline{\overline{C}} \cdot \mathbf{J}_s(\boldsymbol{\rho}), \qquad \zeta = -z-h \tag{7}$$

a source in the three-dimensional space. For the field integral (6) to be bounded, it may be necessary to choose an integration path in the complex z' plane. This can be interpreted as the image source existing in complex space.

B. Image Functions

For the isotropic ground with relative permittivity and permeability ϵ_r, μ_r, the three image functions can be expressed in terms of a two-variable function $f(\alpha, p)$ as [10]

$$f^{\rm TE}(\zeta) = \frac{\mu_r - 1}{\mu_r + 1}\delta(\zeta) + jBf(\mu_r, jB\zeta) \tag{8}$$

$$f^{\rm TM}(\zeta) = -\frac{\epsilon_r - 1}{\epsilon_r + 1}\delta(\zeta) - jBf(\epsilon_r, jB\zeta) \tag{9}$$

$$f_o(\zeta) = -\frac{\epsilon_r^2 - 1}{\epsilon_r(\epsilon_r - \mu_r)}jBf(\epsilon_r, jB\zeta) - \frac{\mu_r^2 - 1}{\mu_r(\mu_r - \epsilon_r)}jBf(\mu_r, jB\zeta) \tag{10}$$

$$B = k_o\sqrt{\mu_r\epsilon_r - 1} \tag{11}$$

and $f_o'(\zeta)$ is the derivative of $f_o(\zeta)$. The function $f(\alpha, p)$ is defined by

$$f(\alpha, p) = -\frac{8\alpha}{\alpha^2 - 1}\sum_{n=1}^{\infty} n\left(\frac{\alpha - 1}{\alpha + 1}\right)^n \frac{J_{2n}(p)}{p}\theta(p), \quad \alpha \ne 1 \tag{12}$$

$$f(1, p) = -2\frac{J_2(p)}{p}\theta(p). \tag{13}$$

Because values of the Bessel functions $J_n(p)$ decrease in magnitude with increasing argument only if p is real, we must choose the location of the image in the complex z plane so that $p = jB\zeta = -jB(z+h)$ is real. The heaviside unit step function $\theta(p)$ guarantees that the image exists only for $p \ge 0$, i.e., that it starts from the mirror image point $z = -h$.

For large absolute values of the parameter α we can simplify the function (12) using known properties of the Bessel function [12]. In fact, for $|\alpha| \to \infty$ we have

$$f(\alpha, p) \to -\frac{8}{\alpha}\sum_{n=1}^{\infty} n\frac{J_{2n}(p)}{p}\theta(p) = \frac{2}{\alpha}g(p)\theta(p) \tag{14}$$

where the function $g(p)$ and its derivative are

$$g(p) = -4\sum_{n=1}^{\infty} n\frac{J_{2n}(p)}{p} = J_1(p) - \int_0^p J_0(p)\,dp \tag{15}$$

$$g'(p) = -\frac{1}{2}[J_0(p) + J_2(p)] = -\frac{J_1(p)}{p}. \tag{16}$$

The function $g(p)$ appears essentially simpler than $f(\alpha, p)$ both as an analytic expression and in its functional dependence on the argument p. As is seen from Fig. 1, $g(p)$ oscillates slightly when approaching the value -1 when p increases. Its extremal values are obtained at the nulls $p_1, p_2, \ldots$ of the function $J_1(p)$ for $p > 0$. The first minimum is $g(p_1) \approx -1.08$ at $p_1 \approx 3.832$.

The Bessel functions satisfy the following integral relations valid for any integer m

$$\int_0^{\infty} \frac{J_2(p)}{p}\,dp = \frac{1}{2}, \quad \int_0^{\infty} J_m(p)\,dp = 1. \tag{17}$$

Applied to the expansion (12), we obtain

$$\int_{-\infty}^{\infty} f(\alpha, p)\,dp = -\frac{2\alpha}{\alpha + 1}, \quad \int_{-\infty}^{\infty} pf(\alpha, p)\,dp = -2\alpha. \tag{18}$$

In some cases, the function $f(\alpha, p)$ can be approximated by a δ function. The form of the approximation

$$f(\alpha, p) \approx -\frac{2\alpha}{\alpha + 1}\delta(p - \alpha - 1) \tag{19}$$

can be found by requiring that the first two moment integrals $\int f(\alpha, p)dp$ and $\int pf(\alpha, p)dp$ are the same on both sides of (19) [7].

III. Geophysical Approximation

A. Asymptotically Exact Images

The image expressions can be simplified under three conditions characteristic to geophysical problems: 1) the frequency is small; 2) the ground is nonmagnetic; and 3) has nonvanishing conductivity. To approximate the previous expressions we set $\mu_r = 1$ and express the complex ϵ_r of the ground as

$$\epsilon_r = \epsilon_{re} + \frac{\sigma}{j\omega\epsilon_o} \tag{20}$$

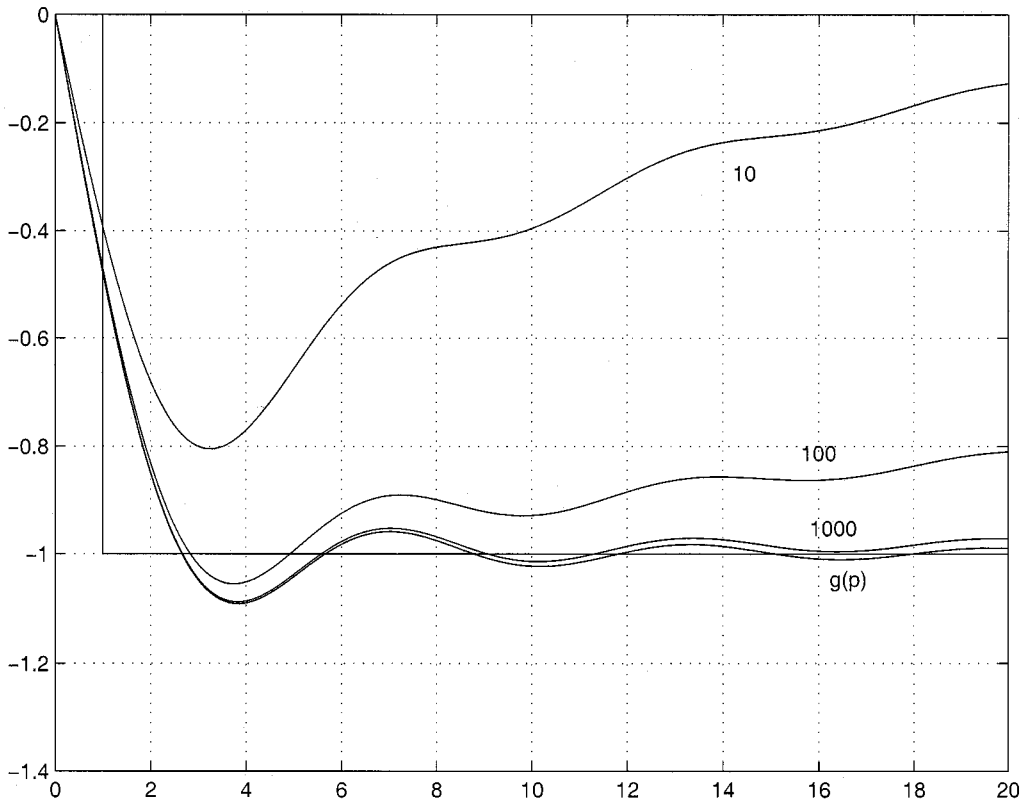

Fig. 1. Graphs of the normalized function $(\alpha/2)f(\alpha, p)$ for different real values of the parameter α. For $\alpha \to \infty$ the limiting function is $g(p)$. It can be approximated by the negative step function $-\theta(p-1)$.

where $\epsilon_{re} > 1$ denotes the real part of the relative permittivity. Further, we write the parameter B as

$$B = k_o\sqrt{\epsilon_r - 1} = \sqrt{-j\omega\mu_o\sigma}\sqrt{1 + j\frac{\omega\epsilon_o}{\sigma}(\epsilon_{re} - 1)}. \quad (21)$$

Assuming now nonvanishing conductivity and small ω so that $\tau = \sigma/\omega\epsilon_o \gg \epsilon_{re}$ is valid, the complex relative permittivity $\epsilon_r \approx -j\tau$ has a large magnitude. On the other hand, the wavenumber parameter B can be approximated by

$$B \approx \sqrt{-j\omega\mu_o\sigma} = k_o\sqrt{-j\tau} \approx k_o\sqrt{\epsilon_r}. \quad (22)$$

Since the magnitude $|B|$ need not be small if σ happens to be large, we make no further assumption at this point.

Let us now find the asymptotic forms for the previous image functions in the limit $|\epsilon_r| \to \infty$. First, the image function f^{TE} does not depend on ϵ_r and is simple enough in its exact form

$$f^{\mathrm{TE}}(\zeta) = jBf(1, jB\zeta) = -2\frac{J_2(jB\zeta)}{\zeta}\theta(jB\zeta). \quad (23)$$

Here and in the sequel, the step function $\theta(jB\zeta)$ has a meaning because, in our assumption, $jB\zeta = p$ is real.

The other image functions depend on ϵ_r through the function $f(\epsilon_r, p)$ and can be approximated for large values of $|\epsilon_r|$ in terms of the function $g(p)$ defined in (16) as

$$\begin{aligned} f^{\mathrm{TM}}(\zeta) &= -\frac{\epsilon_r - 1}{\epsilon_r + 1}\delta(\zeta) - jBf(\epsilon_r, jB\zeta) \\ &\approx -\frac{\epsilon_r - 1}{\epsilon_r + 1}\delta(\zeta) - \frac{2jB}{\epsilon_r}g(jB\zeta)\theta(jB\zeta) \quad (24) \\ f_o(\zeta) &= -\frac{\epsilon_r + 1}{\epsilon_r}jBf(\epsilon_r, jB\zeta) \\ &\approx -\frac{2jB}{\epsilon_r}g(jB\zeta)\theta(jB\zeta) \quad (25) \\ f_o'(\zeta) &\approx -\frac{2jB}{\epsilon_r}[\partial_\zeta g(jB\zeta)]\theta(jB\zeta) \\ &= 2k_o^2 g'(jB\zeta)\theta(jB\zeta). \quad (26) \end{aligned}$$

These expressions for the image functions are asymptotically exact and replace the more elaborate forms (9), (10), valid for general values of ϵ_r. This means saving in computer time.

B. Approximate Images

The previous image expressions can be further simplified by approximating them through simpler functions. The simplest possible functions in an integration are, of course, δ functions. A function with values concentrated enough around some point

can be approximated by a δ function at a suitable location found by equating the first two moments of the function and its δ approximation as was done for the function $f(\alpha, p)$ in (19).

When the image function $f^{\rm TE}(\zeta)$ in (23) is approximated by the δ function through (19) as

$$\begin{aligned} f^{\rm TE}(\zeta) &= jBf(1, jB\zeta) \\ &\approx -jB\delta(p-2) \\ &= -\delta\left(\frac{p}{jB} - \frac{2}{jB}\right) \\ &= -\delta\left(\zeta - \frac{2}{jB}\right) \end{aligned} \tag{27}$$

it is seen to lead to the celebrated Wait's image [1], [3]. This result was also obtained in [5], [7], [10], [19], and [20]. In trying to do the same for the image functions $f^{\rm TM}(\zeta)$ and $f_o(\zeta)$ leads to trouble because the $g(p)$ function is not peaked and rather resembles a step function. However, its derivative can be now approximated by the δ function. Because of (16) and (17) we have

$$\int_0^\infty g'(p)dp = \int_0^\infty pg'(p)\,dp = -1 \tag{28}$$

and the approximation becomes

$$g'(p)\theta(p) = -\frac{J_1(p)}{p} \approx -\delta(p-1) \tag{29}$$

in a manner analogous to that giving Wait's image. Thus, through integration we obtain the step-function approximation for the function $g(p)\theta(p)$ as

$$g(p)\theta(p) \approx -\theta(p-1). \tag{30}$$

These finally lead to the following approximations of the image functions, which forms an extension to Wait's image theory:

$$\begin{aligned} f^{\rm TM}(\zeta) &\approx -\frac{\epsilon_r - 1}{\epsilon_r + 1}\delta(\zeta) - \frac{2jB}{\epsilon_r}g(jB\zeta)\theta(jB\zeta) \\ &\approx -\frac{\epsilon_r - 1}{\epsilon_r + 1}\delta(\zeta) + \frac{2jB}{\epsilon_r}\theta(jB\zeta - 1) \end{aligned} \tag{31}$$

$$f_o(\zeta) \approx -\frac{2k_o^2}{jB}\theta(jB\zeta - 1) \tag{32}$$

$$f_o'(\zeta) \approx -2k_o^2\delta(jB\zeta - 1) = -\frac{2k_o^2}{jB}\delta\left(\zeta - \frac{1}{jB}\right). \tag{33}$$

IV. Approximate Image Expressions

Let us now apply the previous expressions to find image sources corresponding to different source functions $\mathbf{J}(\boldsymbol{\rho})$ at the height h above the interface.

A. Vertical Dipole

A vertical current dipole of the moment IL at height h

$$\mathbf{J}(\mathbf{r}) = \mathbf{u}_z IL\delta(\boldsymbol{\rho})\delta(z-h) \tag{34}$$

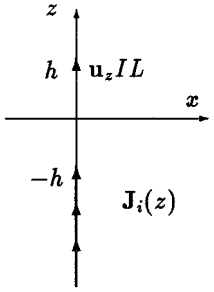

Fig. 2. Image of a vertical dipole consists of a dipole at the mirror image point $z = -h$ and a half-infinite line current obeying the image function $f^{\rm TM}(-z-h)$.

has the image

$$\mathbf{J}_i(\mathbf{r}) = -\mathbf{u}_z IL\delta(\boldsymbol{\rho})f^{\rm TM}(-z-h) \tag{35}$$

which is a half-infinite line current starting from $z = -h$ Fig. 2. When inserting the asymptotically exact function from (24) to the image of the vertical electric dipole (35), we have

$$\begin{aligned} \mathbf{J}_i(\mathbf{r}) \approx{}& \mathbf{u}_z IL\delta(\boldsymbol{\rho}) \\ &\cdot\left[\frac{\epsilon_r - 1}{\epsilon_r + 1}\delta(z+h) + \frac{2jB}{\epsilon_r}\right. \\ &\left.\cdot g(-jB(z+h))\theta(-jB(z+h))\right]. \end{aligned} \tag{36}$$

Replacing now the g function by the negative step function we have the simple approximation

$$\begin{aligned} \mathbf{J}_i(\mathbf{r}) \approx{}& \mathbf{u}_z IL\delta(\boldsymbol{\rho})\left[\frac{\epsilon_r - 1}{\epsilon_r + 1}\delta(z+h) - \frac{2jB}{\epsilon_r}\right. \\ &\left.\cdot\theta(-jB(z+h) - 1)\right] \end{aligned} \tag{37}$$

which is a combination of a dipole at the mirror image point and a constant vertical line current in complex space. One should note that this constant line current does not start from the mirror image point $z = -h$ but, rather, from the complex point $z = -h - 1/jB$.

It is seen that in the limit $\omega \to 0$ the second term vanishes and the first one approaches

$$\mathbf{J}_i(\mathbf{r}) \to \mathbf{u}_z IL\delta(\boldsymbol{\rho})\delta(z+h) \tag{38}$$

which is the reverted geometrical image of the vertical dipole and corresponds to the image in a perfectly conducting (PEC) half-space.

B. Horizontal Source

Applying (7) and (3) to a horizontal surface current source

$$\mathbf{J}(\mathbf{r}) = \mathbf{J}_s(\boldsymbol{\rho})\delta(z-h), \quad \mathbf{u}_z \cdot \mathbf{J}_s = 0 \tag{39}$$

leads to the image source of the form

$$\mathbf{J}_i(\mathbf{r}) = \mathbf{J}_s(\boldsymbol{\rho})f^{\rm TE}(-z-h) - \frac{1}{k_o^2}\mathbf{u}_z[\nabla \cdot \mathbf{J}_s(\boldsymbol{\rho})]f_o'(-z-h). \tag{40}$$

The image is seen to consist of both horizontal and vertical currents, in general. If the original surface current is solenoidal satisfying $\nabla \cdot \mathbf{J}_s(\boldsymbol{\rho}) = 0$, its mirror image is purely horizontal

$$\mathbf{J}_i(\mathbf{r}) = \mathbf{J}_s(\boldsymbol{\rho}) f^{\mathrm{TE}}(-z-h). \tag{41}$$

In this case, the image is also solenoidal. For nonsolenoidal currents there exists concentration of surface charge $\varrho_s(\boldsymbol{\rho})$, which can be expressed from the conservation law as

$$\varrho_s(\boldsymbol{\rho}) = -\frac{1}{j\omega} \nabla \cdot \mathbf{J}_s(\boldsymbol{\rho}) \tag{42}$$

(40) can now be written as

$$\mathbf{J}_i(\mathbf{r}) = \mathbf{J}_s(\boldsymbol{\rho}) f^{\mathrm{TE}}(-z-h) + \frac{j\omega}{k_o^2} \mathbf{u}_z \varrho_s(\boldsymbol{\rho}) f_o'(-z-h). \tag{43}$$

As is seen from the above, the functions $f^{\mathrm{TE}}(\zeta)$ and $f_o'(\zeta)$ give the respective images of the solenoidal current and charge density parts of the horizontal current function.

1) Horizontal Current Segment: As an illustration, let us consider an x-directed line-current segment of length $2a$ and magnitude I (Fig. 3)

$$\mathbf{J}(\mathbf{r}) = \mathbf{u}_x I[\theta(x+a) - \theta(x-a)]\delta(y)\delta(z-h). \tag{44}$$

The corresponding surface charge distribution

$$\varrho_s(\boldsymbol{\rho}) = -\frac{I}{j\omega}[\delta(x+a) - \delta(x-a)]\delta(y) \tag{45}$$

equals two point charges at the ends of the segment. The horizontal image component of the line current

$$\mathbf{J}_{ih}(\mathbf{r}) = \mathbf{u}_x I[\theta(x+a) - \theta(x-a)]\delta(y) f^{\mathrm{TE}}(-z-h) \tag{46}$$

is an half-infinite strip of horizontal surface current in the region $|x| \le a$ (Fig. 3). Under the geophysical approximation (27) we can apply Wait's image theory and replace the current strip by the current line image (Fig. 4)

$$\mathbf{J}_{ih}(\mathbf{r}) \approx -\mathbf{u}_x I[\theta(x+a) - \theta(x-a)]\delta(y)\delta\left(z+h+\frac{2}{jB}\right). \tag{47}$$

As a quick check, for the PEC case ($\sigma \to \infty$, $B \to \infty$), the negative mirror image of the current segment is obtained.

The vertical image component corresponding to the two point charges

$$\mathbf{J}_{iv}(\mathbf{r}) = -\mathbf{u}_z \frac{I}{k_o^2}[\delta(x+a) - \delta(x-a)]\delta(y) f_o'(-z-h) \tag{48}$$

consists of two half-infinite vertical line currents at the edges $x = \pm a$ of the current strip. Applying again the approximate image, the line currents can be replaced by the vertical current dipoles

$$\mathbf{J}_{iv}(\mathbf{r}) \approx \mathbf{u}_z \frac{2I}{jB}[\delta(x+a) - \delta(x-a)]\delta(y)\delta\left(z+h+\frac{1}{jB}\right). \tag{49}$$

For the PEC limit the vertical image of the charges vanishes because $|B| \to \infty$.

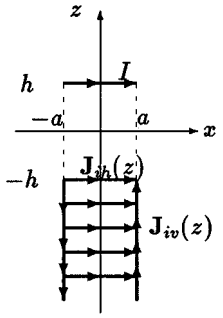

Fig. 3. Image of a horizontal current line segment consists of a horizontal surface current strip and two vertical current lines. They obey the respective image functions $f^{\mathrm{TE}}(-z-h)$ and $f_o'(-z-h)$.

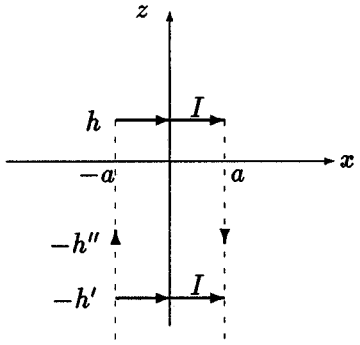

Fig. 4. Approximate image of the horizontal current line segment consists of a horizontal line current image at the depth $z = -h' = -h - 2/jB$ and two vertical image dipoles at the depth $z = -h'' = -h - 1/jB$. Vertical images correspond to the two charges at the endpoints of the original line current.

C. Point Charge

Equations (48) and (49) can be understood as image representations of two point charges $\pm Q$ with $Q = I/j\omega$, occupying the ends $x = \pm a$ of the line current. From these expressions we can identify the image of a single time-harmonic point charge, which although nonphysical as such, appears to be a useful concept when the effect of atmospheric charge accumulation is considered [6]. In fact, the image of the oscillating point charge

$$\varrho(\mathbf{r}) = Q\delta(\boldsymbol{\rho})\delta(z-h) \tag{50}$$

can be expressed as the vertical line current

$$\mathbf{J}_{iq}(\mathbf{r}) = \mathbf{u}_z \frac{j\omega Q}{k_o^2}\delta(\boldsymbol{\rho}) f_o'(-z-h). \tag{51}$$

In the geophysical approximation we can first write the image as the asymptotically exact vertical line current

$$\begin{aligned}\mathbf{J}_{iq}(\mathbf{r}) &\approx \mathbf{u}_z 2j\omega Q\delta(\boldsymbol{\rho}) g'(-jB(z+h)) \\ &= \mathbf{u}_z \frac{2\omega Q}{B}\delta(\boldsymbol{\rho}) \frac{J_1(-jB(z+h))}{z+h}\end{aligned} \tag{52}$$

and in the vertical dipole approximation as

$$\mathbf{J}_{iq}(\mathbf{r}) \approx -\mathbf{u}_z \frac{2\omega Q}{B}\delta(\boldsymbol{\rho})\delta\left(z+h+\frac{1}{jB}\right). \tag{53}$$

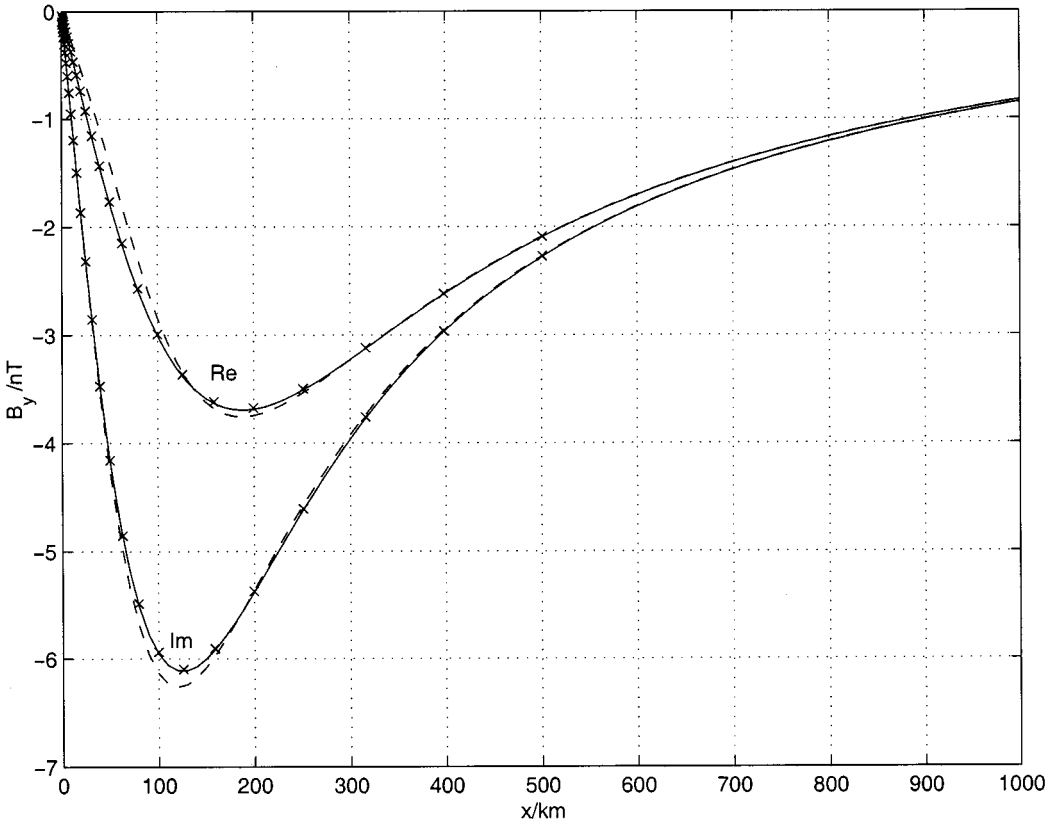

Fig. 5. Real and imaginary components of the field $B_y(x)$ (in nano Teslas) at the ground $z = 0$ due to a current wave in ionosphere for time parameter $T = 20$ s. Crosses: exact computation; solid lines: field from asymptotically exact image; dashed lines: field from δ-approximated image.

V. Numerical Test

To convince the reader on the quite complicated formulas above, a numerical test was made to check the image theory for a typical geophysical problem. A horizontal line current above the earth was assumed with parameter values corresponding to an auroral electrojet current in the ionosphere. The line current was not assumed constant but rather as a wave of the form

$$\mathbf{J}(\mathbf{r}) = \mathbf{u}_y I e^{-jqy} \delta(x)\delta(z-h) \tag{54}$$

with the numerical values $I = 10^5$ A, $h = 100$ km, $q = 10^{-6}$ 1/m. For such a wave the divergence does not vanish and there are accumulating charges along the current. The time period (inverse frequency) of the ELF current was taken to be $T = 20$ s. The conductivity of the homogeneous flat ground was chosen to be $\sigma = 10^{-3}$ $1/\Omega$m. Because fields at the ground may induce in overhead lines currents large enough to saturate transformers resulting in blackouts in power systems, field computation is of practical interest [14], [15].

As was seen above, the image of the current consists of both horizontal and vertical parts. Because the horizontal part is covered by Wait's image, it can be omitted and only the effect of the novel vertical image component is of interest. It is quite easily seen that the magnetic-field component B_y, which is parallel to the original current and Wait's image, is solely caused by the vertical image. Thus, it can be used as an indicator to validate the approximative vertical image component.

Exact values of the component B_y at the surface of the ground were based on a formulation without image concepts [16] and the fast Hankel transform [17] which was applied to actual numerical computation. In Fig. 5 depicting the field values, the points (crosses) corresponding to the exact field are seen to practically coincide with the solid curve representing field values computed with the asymptotically exact image expression. Thus, the asymptotically exact image reproduces the exact results within the accuracy of the figure. The approximate δ-function image (the dashed line) is also seen to give quite good accuracy, which shows us that, in practical computation, it can be relied on for the present values of parameters. Because the δ function approximates the exact image function, one can understand that for such cases when the exact image is not very concentrated, it must lead to errors in field computation to a close range of points. A more detailed discussion on these relations must, however, be left to a subsequent paper.

VI. Conclusion

The well-known complex image method introduced in 1969 by J. R. Wait, applicable to horizontal solenoidal currents above the planar interface of the ground in the LF approximation, was generalized to allow also nonsolenoidal horizontal and vertical currents. All approximate image expressions were derived from the exact image theory introduced in 1984. In the LF approximation, the image expressions were first given an asymptotically exact limiting form, simple enough for accurate compu-

tation. The final approximate image expressions were seen to arise from these as δ and step-function approximations giving Wait's image among the results. The novel image term was verified through a numerical test.

ACKNOWLEDGMENT

The authors would like to thank Prof. K. Nikoskinen and Dr. A. Viljanen for numerous discussions on the problems of this study. They would also like to thank a reviewer for a discussion on references dealing with the history of the complex image concept. An early reference from 1966 as an unpublished report [18] seems to have preceded Prof. Wait's paper. However, these authors were not able to get in touch with this report to verify this fact.

REFERENCES

[1] J. R. Wait, "Image theory of a quasistatic magnetic dipole over a dissipative ground," *Electron. Lett.*, vol. 5, pp. 281–282, June 1969.
[2] J. R. Wait and K. Spies, "On the image representation of the quasistatic fields of a line current source above the ground," *Can. J. Phys.*, vol. 47, pp. 2731–2733, 1969.
[3] J. R. Wait, "Complex image theory—revisited," *IEEE Antennas Propagat. Mag.*, vol. 33, no. 4, pp. 27–29, Aug. 1991.
[4] D. J. Thomson and J. T. Weaver, "The complex image approximation for induction in a multilayered earth," *J. Geophys. Res.*, vol. 80, no. 1, pp. 123–129, Jan. 1975.
[5] I. V. Lindell and E. Alanen, "Exact image theory for the Sommerfeld half-space problem," *IEEE Trans. Antennas Propagat.*, vol. AP-32, pp. 126–133, Feb. 1984.
[6] R. Pirjola and A. Viljanen, "Complex image method for calculating electric and magnetic fields produced by an auroral electrojet of finite length," *Ann. Geophysicae*, vol. 16, pp. 1434–1444, 1998.
[7] I. V. Lindell and K. I. Nikoskinen, "Complex space multipole theory for scattering and diffraction problems," *Radio Sci.*, vol. 22, no. 6, pp. 963–967, Nov. 1987.
[8] P. R. Bannister, "Applications of complex image theory," *Radio Sci.*, vol. 21, pp. 605–616, 1986.
[9] S. F. Mahmoud and A. D. Metwally, "New image representations for dipoles near a dissipative earth," *Radio Sci.*, pt. 1, vol. 16, pp. 1271–1275, 1981.
[10] I. V. Lindell, *Methods for Electromagnetic Field Analysis*, 2nd ed. Oxford, U.K.: Oxford Univ. Press, 1995.
[11] J. T. Weaver, *Mathematical Methods for Geo-Electromagnetic Induction*. Taunton, U.K.: Research Studies, 1994, pp. 63–67.
[12] A. P. Prudnikov, Y. A. Brychkov, and O. I. Marichev, *Integrals and Series, Volume 2: Special Functions*. New York: Gordon Breach, 1986.
[13] I. V. Lindell, "Delta function expansions, complex delta functions and the steepest descent method," *Amer. J. Phys.*, vol. 61, no. 5, pp. 438–442, 1993.
[14] J. G. Kappenman and V. D. Albertson, "Bracing for the geomagnetic storms," *IEEE Spectrum*, vol. 27, no. 3, pp. 27–33, Mar. 1990.
[15] D. H. Boteler, R. Pirjola, and H. Nevanlinna, "The effects of geomagnetic disturbances on electrical systems at the earth's surface," *Adv. Space Res.*, vol. 22, no. 1, pp. 17–27, 1998.
[16] R. Pirjola, "Electromagnetic induction in the earth by a line current harmonic in time and space," *Geophysica*, vol. 21, no. 2, pp. 127–143, 1985.
[17] H. K. Johansen and K. Sorensen, "Fast Hankel transforms," *Geophys. Prospect.*, vol. 27, pp. 876–901, 1979.
[18] "Westinghouse Electric Co. Report,", Boulder, CO, 1966.
[19] I. V. Lindell and E. Alanen, "Exact image theory for the Sommerfeld half-space problem," *IEEE Trans. Antennas Propagat.*, vol. AP-32, pp. 841–884, Aug. 1984.
[20] ——, "Exact image theory for the Sommerfeld half-space problem," *IEEE Trans. Antennas Propagat.*, vol. AP-32, pp. 1027–1032, Oct. 1984.
[21] S. F. Mahmoud and A. D. Metwally, "New image representations for dipoles near a dissipative earth," *Radio Sci.*, pt. 2, vol. 16, pp. 1277–1283, 1981.

Ismo V. Lindell (S'68–M'69–SM'83–F'90) was born in 1939. He received the Dr.Tech. (Ph.D.) degree from Helsinki University of Technology (HUT), Espoo, Finland, in 1971.

Currently, he is a Professor of electromagnetic theory at the Electromagnetics Laboratory, HUT, and at the same time holds a research position of Professor of the Academy of Finland, until 2001. He has authored and coauthored scientific papers and books, including *Methods for Electromagnetic Field Analysis* (New York: IEEE Press, 1995, 2nd ed.), *Electromagnetic Waves in Chiral and Bi-Isotropic Media* (Norwood, MA: Artech House, 1994), and *History of Electrical Engineering* (Espoo, Finland: Otatieto, 1994, in Finnish).

Dr. Lindell received the IEEE S. A. Schelkunoff Prize (1987) and the IEE Maxwell Premium (1997 and 1998). He is Commission B Chairman of the URSI National Committee of Finland.

Jari J. Hänninen was born in Jyväskylä, Finland, in 1966. He received the M.Sc. degree in electrical engineering at the Helsinki University of Technology (HUT), Espoo, Finland, in 1991. He is currently working toward the D.Sc. (Tech.) degree at the HUT Electromagnetics Laboratory.

From 1991 to 1998, he was with the Finnish Defence Forces.

Risto Pirjola was born in Helsinki, Finland, on February 13, 1950. He received the B.Sc. and M.Sc. degrees in mathematics in 1970 and 1971, respectively, and the Ph.D. degree in theoretical physics in 1982, all from the University of Helsinki, Finland.

From 1970 to 1972, he was an Assistant with the Department of Theoretical Physics, University of Helsinki. From 1973 to 1978, he served as a Research Scientist with the General Direction of Posts and Telegraphs of Finland, Helsinki. Since 1978, he has been a Scientist at the Geophysical Research Division of the Finnish Meteorological Institute (FMI), Helsinki. His research interests have mainly been concentrated on the modeling of the geoelectromagnetic variation field observed at the earth's surface at auroral latitudes and on studies of space weather effects on the ground, i.e., geomagnetically induced currents in power transmission systems and pipelines. From 1992 to 1997, he was the project manager of FMIs contributions to international planetary exploration projects.

Dr. Pirjola is an Official Member of Commission E of URSI since 1976. He is a Chairman of the URSI-E Working Group on "geoelectromagnetic disturbances and their effects on technological systems."